Internal Conrotation and Disrotation in $H_2BCH_2BH_2$ and Diborylmethane 1,3 H Exchange

RUSLAN M. MINYAEV,[1] WOLFGANG QUAPP,[2] GOVINDAN SUBRAMANIAN,[3] PAUL VON R. SCHLEYER,[3] YIRONG MO[3]

[1]*Institute of Physical and Organic Chemistry, Rostov State University, 194/3 Stachka Avenue, Rostov-on-Don 344104, Russia,*
[2]*Mathematical Institute, Leipzig University, Augustsplatz, D-04109 Leipzig, Germany,*
[3]*Computer Chemie Centrum, Institut für Organische Chemie, Universität Erlangen–Nürnberg, Henkestrasse 42, D-91054 Erlangen, Germany*

Received 6 September 1996; accepted 19 May 1997

ABSTRACT: The paths of correlated internal disrotation (barrier less than 0.4 kcal/mol) and conrotation (barrier around 1.9 kcal/mol) of the two BH_2 groups in $H_2BCH_2BH_2$ have been computed employing *ab initio* [MP2(full)/6–31G**] and density functional theory (Becke3LYP/6–311 + G**) methods. Two B—C ⋯ B(p) hyperconjugative interactions stabilize the C_s symmetric $H_2BCH_2BH_2$ isomer (**1**). The B—C ⋯ B(p) hyperconjugative stabilization, evaluated by homodesmotic reactions and using the orbital deletion procedure (which ''deactivates'' the ''vacant'' born p orbital), is less than 6 kcal/mol in diborylmethane. The B—C ⋯ B(p) stabilization is shown to be remarkably large in $C_4B_6H_{10}$ (*Td*). At MP2(fu)/6–31G**, disproportionation into **1** and methane is only 5.6 kcal/mol exothermic. The 1,3 H exchange in diborylmethane is an asynchronous process and proceeds via a doubly bridged cyclic intermediate with 9.3 kcal/mol barrier. Structures with ''planar tetracoordinate'' carbon are stabilized considerably by BH_2 substituents, but they are still high in energy.
 J Comput Chem **18**: 1792–1803, 1997

Keywords: diborylmethane; conrotation and disrotation; 1,3 H exchange; orbital deletion procedure; gradient line reaction path

Correspondence to: G. Subramanian; E-mail: mrm@ipoc.rostov-na-donu.su

This work is dedicated to Professor Roald Hoffmann on the occasion of his 60th birthday.

CCC 0192-8651 / 97 / 141792-12

Introduction

According to the Woodward–Hoffmann rules,[1] the allowed electrocyclic ring closure reactions of polyenes follow either conrotatory or disrotatory pathways. However, the motions of the terminal groups in the ground state of polyenes are both disrotatory and conrotatory. This is shown, for example, by the vibrational assignments of *trans*- and *s-cis*-1,3-butadiene.[2–4] According to experimental data,[5] the correlated thermal cis-trans isomerization of both the terminal—CH(D) groups in 1,4-dideuterio-1,3-butadienes is more rapid than the single rotation process. Similarly, internal correlated conrotations of the two equivalent terminal groups are suggested to occur in the prop-2-yl cation,[6] triplet trimethylene,[7] silylenes,[8] and other molecules.[9] This raises an interesting question: can separate correlated internal disrotation and conrotation (without ring closure) with different transition structures (and different energy barriers) exist in a molecule with two equivalent rotors? The aim of the present article is to examine the simple system, diborylmethane (**1**–**4**, Fig. 1) with two equivalent BH_2 rotors, in this context. Prior theoretical calculations on **1**–**4** at HF/4–31G predicted **3** to be more stable than **1**, **2**, and **4**.[10] However, the nature of the stationary points were not characterized. In addition, we examine the doubly bridged ring closed structure (**5**) that might serve as an intermediate for 1,3 hydrogen exchange (**6**, **7**) in diborylmethane (**1**). Furthermore, the electronic effects of two borons, stabilizing a ''planar tetracoordinate'' carbon[11] prompted us to also investigate such alternatives (**8**–**10**) on the $H_2BCH_2BH_2$ potential energy surface (PES). Attention is also called to the isoelectronic $C_3H_6^{2+}$ system,[12] where some analogous structural features were considered.

Methods

Single-determinant spin-restricted Hartree–Fock (HF) calculations were performed using the Gaussian 94 program[13] employing standard 6–31G** basis sets[14] and optimization thresholds. However, transition structures were recalculated with the ''tight'' option. Further refinement at MP2(full)/

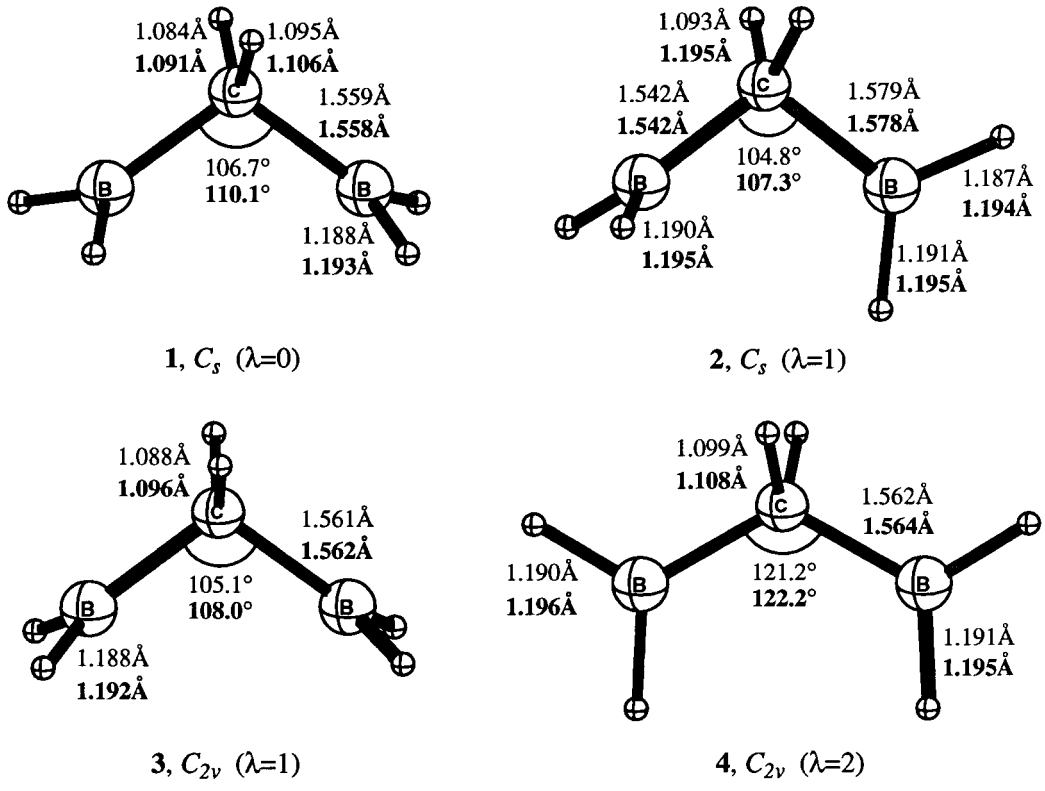

FIGURE 1. MP2(full)/6–31G** and Becke3LYP/6–311+G** (in bold) optimized geometries (bond length in Ångströms and bond angles in degrees) for **1**–**4**.

6–31G** (all electrons were considered in the MP2 treatment of electron correlation) and Becke3LYP/6–311 + G** (B3LYP) levels were employed.[15] Analytical second derivatives[16] established the nature of all stationary points at HF/6–31G**, MP2(full)/6–31G**, and B3LYP levels. Scaled zero-point energies[17] are used to correct the relative energies. The calculated energies and geometries are given in Table I and Figure 1 along with the number of negative Hessian eigenvalues (λ) in parentheses. Unless specified, all discussions are based on the MP2 results. The torsional angles α and β of **1**–**4** (used in Fig. 2) are defined relative to **4** and correspond to the $H^4B^1CB^2$ and $H^6B^2CB^1$ dihedral angles (see Scheme 1 for atom numbering), respectively. Thus, when the H^4 atom eclipses the opposite B^2, $\alpha = 0°$ (i.e., the $H^4B^1CB^2$ dihedral angle is 0°). Angle β, which involves the hydrogen H^6, is defined similar to α. Thus, structure **4** corresponds to $\alpha = \beta = 0°$. A positive value of α corresponds to a clockwise rotation of the BH_2 group as viewed in the B^1C direction.

Results and Discussion

The $H_2BCH_2BH_2$ C_s structure **1**, with two BH_2 groups twisted around the C–B bonds by 68° (the corresponding $H^4B^1CB^2$ and $H^6B^2CB^1$ dihedral angles in **1a** are 62.9° and −62.9° at B3LYP) is a minimum ($\lambda = 0$). Structures **2** and **3** correspond to transition states ($\lambda = 1$) and **4** to an index two ($\lambda = 2$) stationary point (Fig. 1, Table I). No C_2 conformation of acyclic $H_2BCH_2BH_2$ was a stationary point; many attempts to optimize such a conformation at various theoretical levels, always lead to the C_{2v} saddle point ($\lambda = 1$), **3**, instead. As seen from the relative energies of **1**–**4** in Table I, the terminal BH_2 groups in diborylmethane "twist" back and forth (see Scheme 1 and especially Scheme 2) very rapidly, resulting in an essential C_{2v} symmetry in a basin of conformations with approximately constant energy. In contrast, MP4SDTQ/6–3G*//HF/6–31G* calculations on the isoelectronic $C_3H_6^{2+}$ predicted the planar–planar conformation (structurally similar to **4**) to be 6.5 kcal/mol more favored than the planar–perpendicular (structurally similar to **2**) arrangement.[12]

Conrotation of two BH_2 Groups

The coplanar–perpendicular transition structure (TS) **2** for the internal conrotation of the BH_2 groups is fourfold degenerate (Fig. 2a,b). The calculated barrier for **1** ⇒ **2** ⇒ **1** is 1.90 kcal/mol at MP2 and 1.71 kcal/mol at B3LYP (Table I).

TABLE I.
Total (hartrees), Relative (ΔE, kcal/mol) and Zero-Point Energies (ZPE kcal/mol), Number of Negative Eigenvalues (λ), Imaginary or Smallest Frequency ($i\nu/\nu_1$, cm^{-1}) for CB_2H_6 Isomers at MP2(full)/6–31G (MP2) and Becke3LYP/6–311+G** (B3LYP) Levels.**

		Total Energy		ΔE[a]		ZPE (λ)		$i\nu/\nu_1$	
Structure	Sym.	MP2	B3LYP	MP2	B3LYP	MP2	B3LYP	MP2	B3LYP
1	C_s	−91.03050	−91.40863	0.00	0.00	44.0 (0)	42.1 (0)	131.1	160.6
2	C_s	−91.02672	−91.40530	1.90	1.71	43.5 (1)	41.7 (1)	*i*230.6	*i*230.7
3	C_{2v}	−91.03033	−91.40817	0.11	0.38	44.0 (1)	42.2 (1)	*i*111.3	*i*142.3
4	C_{2v}	−91.02004	−91.39929	5.34	4.71	42.7 (2)	40.9 (2)	*i*325.3, *i*119.8	*i*313.3, *i*110.9
5	C_{2v}	−91.02292	−91.39812	6.45	7.94	45.8 (0)	43.5 (0)	534.5	463.9
6	C_1	−91.01632	−91.39434	9.27	9.16	44.4 (1)	42.3 (1)	*i*504.4	*i*426.3
7	C_2	−91.01488	b	9.71	—	43.9 (2)	—	*i*440.0, *i*426.8	
8	C_{2v}	−90.84729	−91.23509	110.64	111.01	39.4 (4)	44.3 (3)	*i*2505.0, *i*1838.0 *i*783.0, *i*590.5	*i*1830.7, *i*679.9 *i*595.5,
9	C_{2v}	−90.93474	−91.32142	57.36	52.04	41.1 (3)	39.3 (1)	*i*1046.7, *i*676.5 *i*152.8	*i*1184.3
10	C_{2v}	−90.89214	−91.28314	83.16	75.39	40.1 (3)	38.6 (3)	*i*1468.2, *i*911.8, *i*699.6	*i*1332.9, *i*894.3 *i*554.8

[a] Includes ZPE scaled by 0.94 for MP2 and 0.96 for B3LYP values.
[b] Geometry optimization starting from the MP2 structure converged to **3**.

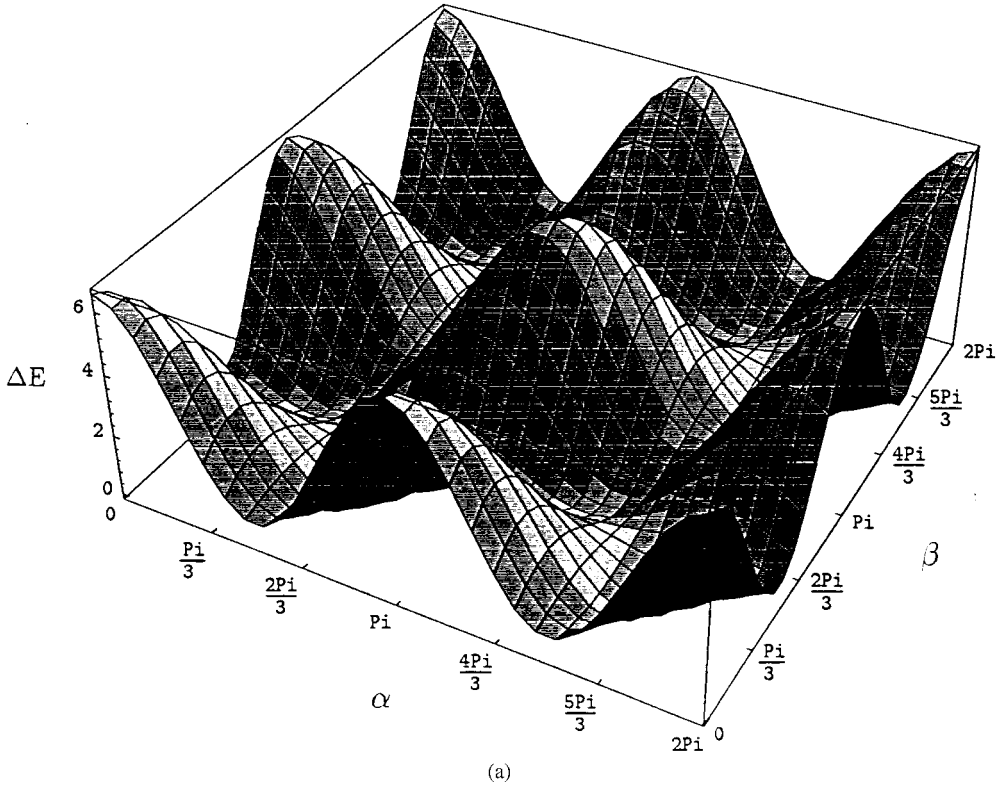

(a)

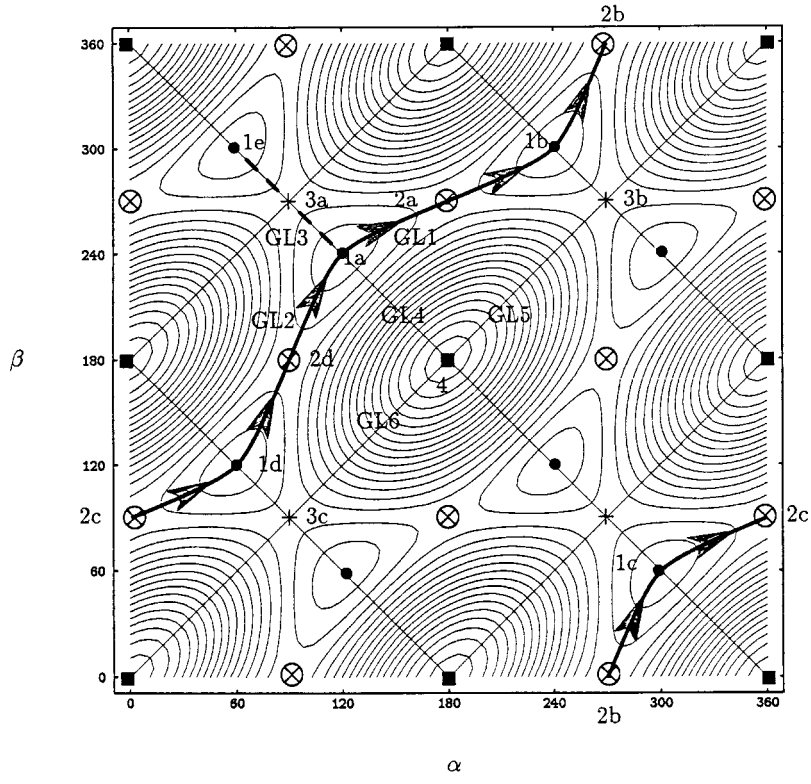

(b)

FIGURE 2. Schematic 3- (**2a**) and 2-dimensional map (**2b**) of the $H_2BCH_2BH_2$ PES based on the torsional angles α and β defined as zero for **4**. (•) Minima **1**; (+, ⊗) designated TSs **2** and **3**, respectively, (■) second index ($\lambda = 2$) critical points **4**. Equipotential lines are thin. The bold continuous and dashed lines designate conrotatory and disrotatory reaction pathways, respectively.

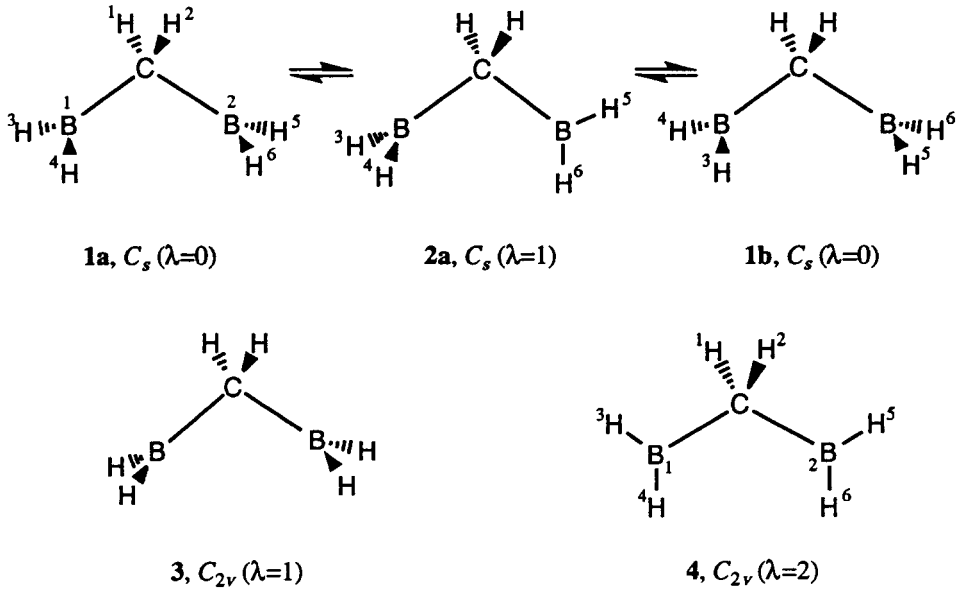

SCHEME 1. Conrotation of the two BH_2 groups.

B(p)⋯C—H hyperconjugation evidently is responsible for the stabilization of the C_s conformation (**1**), because the C–H^1 bonds align with the vacant p orbitals (p) of both boron atoms. [The $HCB^1(p)$ torsional angle is only 2°; the vacant p orbital on boron was assumed to be perpendicular and bisect the $H^3B^1CH^4$ bisector plane.] A similar interaction is also observed in the stable *chiral* twisted conformation (C_2) of the methyl groups in the prop-2-yl cation, where each p-orbital lobe of the central carbon hyperconjugates with the C—H bond of the terminal methyl group.[6]

As shown in Scheme 1, both the BH_2 groups participate in correlated conrotatory motion. The 3-dimensional surface and the 2-dimensional map of the $H_2BCH_2BH_2$ internal rotation PES are illustrated in Figure 2. The internal conrotation occurs along a gradient line reaction path (GLRP)[18] from the saddle point **2a** (the notations **a**–**d** affixed to the structure numbers indicate equivalent conformational arrangements) tangential to the transition vector and enters minimum **1a**. Note that **2a** is tangential to the conrotatory Hessian eigenvector corresponding to the second positive frequency [$\nu_2(A'') = 206.8$ cm^{-1}] and disrotatory mode [$\nu_1(A') = 131.1$ cm^{-1}] of minimum **1** as depicted in Figure 3. The transition vector of **2a** correlates with the conrotatory Hessian eigenvector of **1a**.

The complete four-step sequence is shown by solid lines in Figure 2a. This includes TSs **2a**–**d** and consists of gradient lines connecting neighboring stationary points **1a** ⇔ **2a** ⇔ **1b** ⇔ **2b** ⇔ **1c** ⇔ **2c** ⇔ **1d** ⇔ **2d** ⇔ **1a**. Thus, the internal conrotation occurs along the GLRP tangential to the Hes-

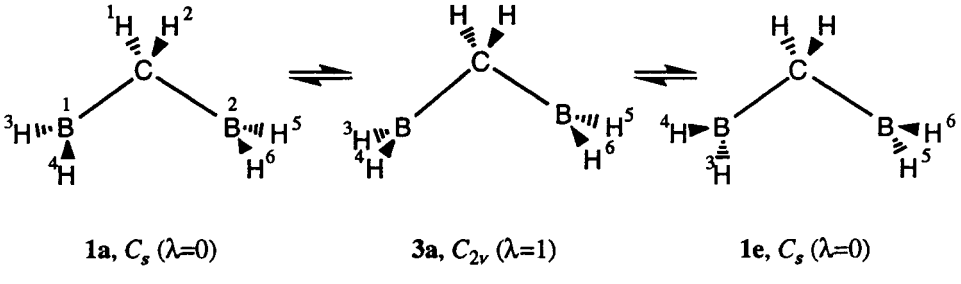

SCHEME 2. Disrotation of the two BH_2 groups.

sian eigenvector, corresponding to the conrotatory mode rather than to the softer (lower energy) disrotatory mode. This is in contrast to the assumption of Fukui[19] that the reaction path is always tangential to the softest mode, which in this case corresponds to the $\nu_1(A') = 131.1\ cm^{-1}$ frequency at MP2(full)/6–31G**.

Disrotation of Two BH_2 Groups

In contrast to the conrotatory pathway, internal disrotation of **1a** occurs through the perpendicular–perpendicular transition structure, **3a** (C_{2v}, Scheme 2). The calculated barrier is considerably smaller than for the conrotation and depends negligibly on basis sets and correlation energy [0.10 at HF/6–31G**; 0.11 at MP2(full)/6–31G**, and 0.38 kcal/mol at B3LYP]. Despite the very small disrotation energy barrier, TS **3** is distinctive (Table I): the energy and all its geometrical parameters differ from those of other configurations. The internal disrotation following the transition vector of **3a** evolves along the GLRP that enters minimum **1a** tangentially to the Hessian eigenvector of the smallest eigenvalue [the disrotatory mode of the smallest frequency ($\nu_1(A') = 131.1\ cm^{-1}$)]. The transition vector and the Hessian eigenvector corresponding to the disrotatory (softest) mode of TS **3** is shown in Figure 4. Comparison of Figure 4 with Figure 3 indicates that both the disrotatory and conrotatory modes of **1** could be fully correlated. The coplanar–coplanar conformation **4** (C_{2v})

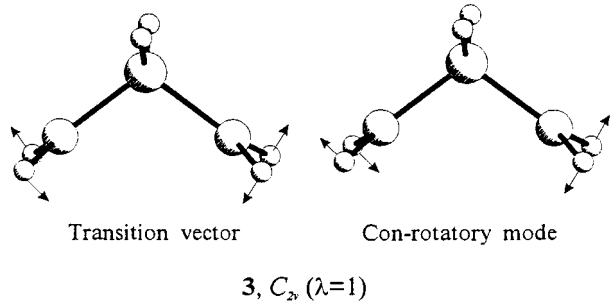

FIGURE 4. The shape of the conrotation [$i\nu(B_1) = 111.3\ cm^{-1}$] and the conrotatory mode corresponding to the smallest positive frequency [$\nu(A_2) = 239.6\ cm^{-1}$] of **3**. Arrows denote the components of the corresponding mode.

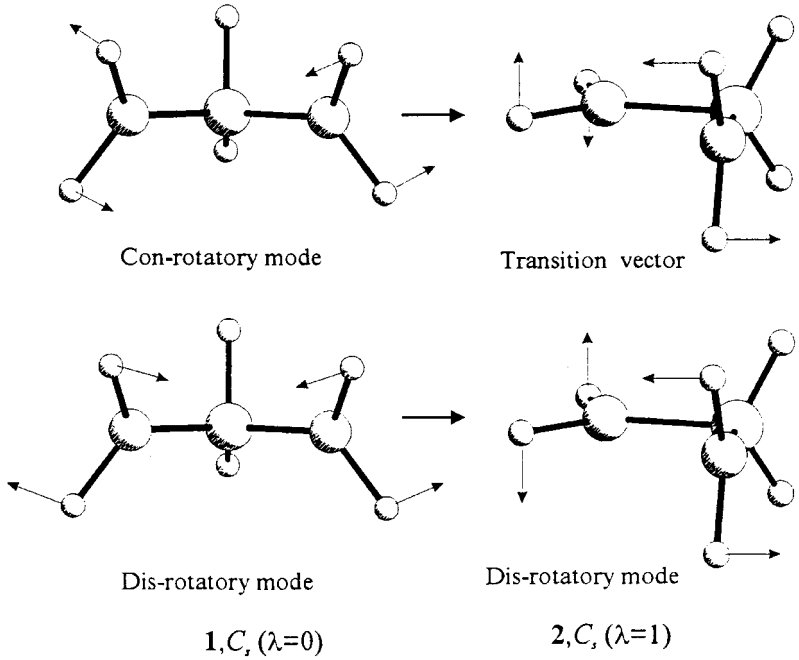

FIGURE 3. Correlation of con- and distrotatory modes for minimum **1** and transition state **2** structures computed at MP2(full) / 6–31G**. Arrows denote the components of the corresponding mode. Conrotatory and disrotatory modes fo **1** have frequencies $\nu_2(A'') = 206.8\ cm^{-1}$ and $\nu_1(A') = 131.1\ cm^{-1}$, respectively. The imaginary and the smallest positive (corresponding to the disrotatory mode) frequencies of **2** are *i*230.6 and 165.1 cm^{-1}, respectively.

is a second-order stationary point ($\lambda = 2$)[20] due to the unfavorable conformations of both BH_2 groups. The two imaginary frequencies in **4** correspond to the disrotation and conrotation motions of the terminal BH_2 groups (Table I).

Topology and Gradient Lines of Rotational PES

Around each minimum **1** (e.g., **1a** in Fig. 2) there are two equivalent conrotatory TSs (**2a** and **2d**) and one disrotatory TS (**3a**). Each of the conrotatory TSs (**2a**, **2d**) is linked with minimum **1a** by two gradient lines (GL1 and GL2, Fig. 2). GL3 and GL4, corresponding to disrotation of the BH_2 groups, link minimum **1a** with the disrotatory TS **3a** (GL3) and with the second order ($\lambda = 2$) stationary point **4** (GL4). In turn, **4** is connected to saddle points **3b** and **3c** by GL5 and GL6 (conrotatory motion). These descriptions are corroborated by analysis of the Hessian eigenvectors corresponding to the negative eigenvalues (Fig. 5).

The conrotatory eigenvector [$\nu_2(A_2) = -119.8$ cm^{-1}] of **4** correlates with the transition vector of **3b**, whereas the disrotatory eigenvector [$\nu_1(B_1) = -325.3$ cm^{-1}] of **4** correlates with the Hessian eigenvector with the smallest positive eigenvalue [$\nu_1(B_1) = 111.3$ cm^{-1}] of TS **3b**. The total distribution of critical points and topology of the rotational PES represented in Figure 2 are indeed consistent with the Morse inequalities[21]:

$$
\begin{aligned}
M_k &\geq B_k \\
M_k - M_{k-1} + \cdots + (-1)^k M_0 & \\
\geq B_k - B_{k-1} + \cdots + (-1)^k B_0, &\qquad k = 0, 1, 2, \ldots; \\
M_n - M_{n-1} + \cdots + (-1)^n M_0 & \\
\geq B_n - B_{n-1} + \cdots + (-1)^n B_0, &
\end{aligned}
$$

where M_k is the number of nondegenerate stationary points with $\lambda = k$ for the adiabatic potential function $E(X) \in C^2$ mapping $R^n \rightarrow R$ ($\forall X \in D$); B_k is the Betti number of rank k for the open region D; n is the dimension of D ($n = 3N - 6$ where N is the number of atoms in the molecule); and the function $E(X)$ must be limited below in D and it must be strictly increasing on the boundary of D. Obviously all these restrictions are satisfied for the PES in the region of angles α and β. Because the largest value of λ is 2, we can always choose a region $D \subseteq R^n$ that is homologous to a 2-dimensional torus and does not contain critical points with $\lambda > 2$. In such a case, the Betti numbers are $B_0 = 1$, $B_1 = 2$, $B_2 = 1$.[22] Taking into account the values $M_2 = 4$, $M_1 = 12$, and $M_0 = 8$ (see Fig. 2), the Morse relations written as,

$$
\begin{gathered}
8 > 1, \quad 12 > 0, \quad 4 > 2; \\
12 - 8 > 0; \\
4 - 12 + 8 = 0,
\end{gathered}
$$

are satisfied. Hence, the topological structure of the $H_2BCH_2BH_2$ PES presented in Figure 2 is consistent with the Morse relationship.

Hyperconjugation in $H_2BCH_2BH_2$

The relatively small activation barriers for both the conrotation and disrotation of the terminal BH_2 groups in **1**–**4** are not direct measures of the hyperconjugation energy involving the empty boron p orbital. The recently proposed orbital deletion procedure (ODP)[23] was employed to evaluate the hyperconjugative stabilization in diborylmethane. The hyperconjugation in such systems containing tricoordinate boron atoms can be described as a perturbation due to ionic resonance

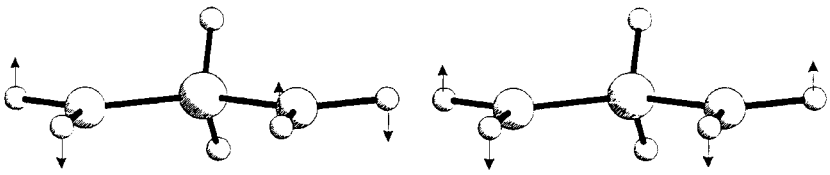

FIGURE 5. The shape of the conrotation [$i\nu(A_2) = 119.8$ cm^{-1}] and the disrotatory [$i\nu(B_1) = 325.3$ cm^{-1}] modes corresponding to the two imaginary frequencies of **4**. Arrows denote the components of the corresponding mode.

contributions to the strictly localized structure. In this hypothetical localized structure, the electron occupation in the empty p atomic orbital (AO) on boron is strictly zero. That is, the hyperconjugation energy (HCE) corresponds to the difference between the energy of the normal structure and that where the ''formally'' hyperconjugating p AO on boron is deleted. Because the ODP method can be applied only within the framework of HF theory at present, we evaluated the hyperconjugation energies for structures **1**–**4** at HF/6–311 + G**//B3LYP/6–311 + G**; local planarity was also imposed for the terminal BH_2 moieties. These approximations had little influence on the relative energies. Relative to **1**, the relevant HF energies of **2**–**4** (without ODP) are 1.54, 0.11, and 4.33 kcal/mol, i.e. close to the B3LYP values.

The two boryl groups in diborylmethane hyperconjugate independently: the net effect is additive.[12,24] This is demonstrated for structures **2** and **4**, where the ''formally vacant'' boron p orbital was deleted initially on only one of the boron centers by the ODP. Table II shows the hyperconjugation energy contribution from each BH_2 group. Then the ''vacant'' p orbital on other boron was deleted instead. The total hyperconjugation energy due to the separate deletion of the vacant p orbitals is also given in Table II. Finally, the vacant p orbitals on both the boron centers were deleted simultaneously; the corresponding hyperconjugation energies are given in parentheses in Table II.

TABLE II.
Hyperconjugation Energies Via ODP at HF/6–311+G//B3LYP/6–311+G****

No.	Sym.	Staggered[a]	Eclipsed[b]	Total (Sum)
1	C_s	−6.0		−12.0
2	C_s	−5.8	−3.7	−9.5 (−9.5)[c]
3	C_{2v}	−6.0		−12.0
4	C_{2v}		−3.4	−6.8 (−6.6)[c]
$H_3C—BH_2$	C_s	−4.4		
$H_3C—BH_2$	C_s		−3.9	

[a]The BH_2 group is perpendicular to the C–B bond opposite.
[b]The BH_2 group is in the plane of the opposite C–H bond.
[c]The hyperconjugation energies for **2** and **4** are −9.5 and −6.6 kcal/mol, respectively, when the vacant p orbitals of both borons are deleted simultaneously rather than successively.

As seen from Table II, the contribution of the ''staggered'' BH_2 is over 2kcal/mol larger than the ''eclipsed.'' In a staggered BH_2 (the BH_2 group is perpendicular to the opposite C–B bond), the empty boron p orbital hyperconjugates with the opposite C—B bond, but with an eclipsed BH_2 the empty boron p orbital only hyperconjugates with the neighboring C—H bonds. Note that the latter contribution (−3.7 kcal/mol in **2**) is close to that of $H_3C—BH_2$ (−3.9 kcal/mol) in the eclipsed form. Because the electronegativity of boron is lower than that of hydrogen, the C—B bond donates electrons more effectively to the vacant boron p orbital than the C—H bond. The hyperconjugation energy of **2** agrees well with that obtained from the sum of the staggered and eclipsed contributions of **1** and **3**. While the hyperconjugation energy for **1** and **3** is the same, **1** is preferred by 0.38 kcal/mol (B3LYP) over **3**. This small difference is due to other effects (e.g., the interactions among the hydrogens).

$$H_3C—BH_3^- + BH_3 \rightarrow H_3C—BH_2 + BH_4^- . \quad (1)$$

As a check of the hyperconjugation energies evaluated employing the ODP, we computed the homodesmotic eq. (1) (without ODP). At the HF//6–311 + G**//B3LYP/6–311 + G** level employed for ODP, Eq. (1) is 7.1 kcal/mol exothermic [5.8 kcal/mol at MP2(full)/6–31G**//MP2(full)/6–31G**]. The difference between the hyperconjugation energy evaluated using eq. (1) and that obtained from ODP (4.4 kcal/mol, Table II), is also attributed to the weaker C—B σ bond in $CH_3BH_3^-$ (1.656Å at B3LYP/6–311 + G**) as compared to that in CH_3BH_2 (1.554 Å).

$$2\,CH_3BH_2(C_s) \rightarrow H_2BCH_2BH_2\,(\mathbf{1}, C_s) + CH_4\,(Td) \quad (2)$$

Equation (2) also evaluates the stabilization energy in **1**, due to the interaction of the two geminal BH_2 groups. Accordingly, the reaction is exothermic by 5.6 kcal/mol at MP2 and 4.0 kcal/mol at B3LYP (2.8 kcal/mol at HF/6–311 + G**//B3LYP/6–311 + G** without ODP). While eq. (2) is also influenced by effects other than hyperconjugation, the energies are comparable to the ODP evaluation.

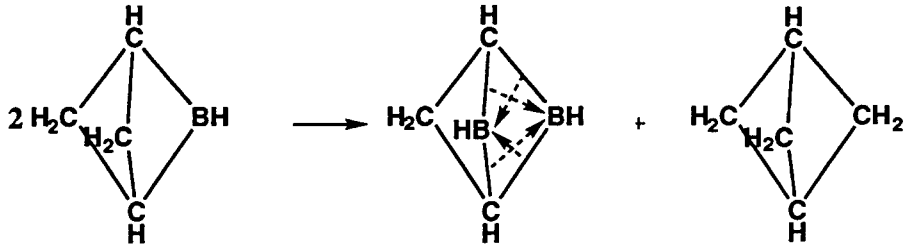

-18.4 kcal/mol at MP2(fc)/6-31+G* (3)

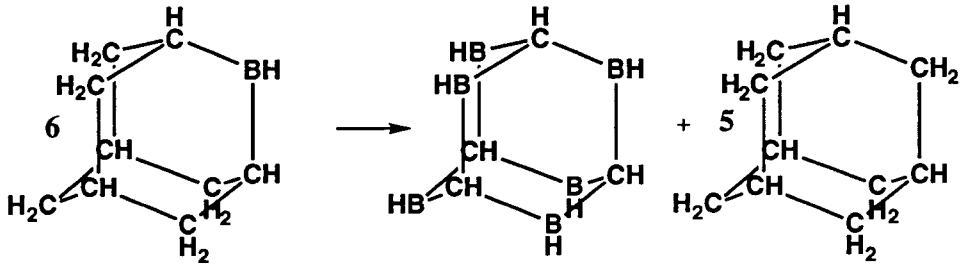

-104.7 kcal/mol at MP2(fc)/6-31G* (4)

The importance of B–C ⋯ B(p) hyperconjugation in other related molecules is demonstrated from the remarkably large computed homodesmotic reaction energies [eqs. (3), (4)]. These formal exchanges compare molecules with more than one boron to reference systems that have only one boron each. Because there are four B—C ⋯ B(p) hyperconjugative interactions in $C_3B_2H_6$ [eq. (3)] and 24 such interactions in $C_4B_6H_{10}^{25}$ [eq. (4)], the energy of each B—C ⋯ B(p) interaction is approximately 4.5 kcal/mol, assuming the strain effects to be similar for all the species. This value is in qualitative agreement with the 6.0 kcal/mol B—C ⋯ B(p) hyperconjugation energy evaluated using ODP for diborylmethane (Table II), considering the difference in dihedral angles between the interacting B–C and B(p) moieties in the molecules in eqs. (3) and (4).

Cyclic Isomer 5 and 1,3 H Exchange

Like borane itself, alkyl-substituted boranes have rather large dimerization energies[26] as computed from eq. (5) (−36.4 kcal/mol at MP2 and −29.2 kcal/mol at B3LYP). However, the cyclization of **1** (which can be regarded as an ''internal dimerization'') would require the cyclic form **5** to have a small BCB angle as evident from the endothermicity of eq. (6) (7.4 and 7.2 kcal/mol at MP2 and B3LYP, respectively). Nevertheless, **5** proves to be a minimum ($\lambda = 0$) and only 6.45 kcal/mol (7.94 kcal/mol at B3LYP) less stable than **1**.

$$2H_3CBH_2\ (C_s) \rightarrow H_3C(H)B(\mu\text{-}H)_2B(H)CH_3\ (C_{2h}) \quad (5)$$

$$C_3H_6\ (D_{3h}) + H_3C(H)B(\mu\text{-}H)_2B(H)CH_3\ (C_{2h}) \rightarrow \mathbf{5}\ (C_{2v}) + H_3C(CH_2)_2CH_3\ (C_2) \quad (6)$$

The B—H—B bridge [1.351 Å; Wiberg bond index (WBI) = 0.473] and the B–B distances (1.608 Å; WBI = 0.659) in the doubly bridged minimum **5**, as compared to diborane [B–H = 1.304 Å, WBI = 0.482; B–B = 1.751Å, WBI = 0.629 at MP2(full)/6–31G**] quantifies the strength of the two 3c-2e B—H—B bonds. Furthermore, while the B–B distance in **5** is much shorter than in **1** (2.502 Å), the C—B bonds are longer than in **1** (1.577 Å). The 6.5 kcal/mol energy difference between **5** and **1** is rather low, despite the destabilization (''strain'') due to the small B—C—B angle.

The doubly bridged minimum (**5**) can also lead to 1,3 H exchange. In principle, **5** might be formed from **1** by conrotation. However, the transition

structure **6** connecting **1** and **5** has C_1 symmetry and is 9.2 kcal/mol higher in energy than **1** at both the MP2 and B3LYP (Table I). The preference of **6** over the symmetrical C_2 structure **7** (a second-order saddle point with $\lambda = 2$ at MP2) clearly suggests that the 1,3 H exchange is not a synchronous process because only one hydrogen atom in **6** bridges (unsymmetrically), while the other (1.224 Å at MP2) still remains terminal. The B—H—B distances in transition structure **6** (1.289 Å, 1.444 Å [not shown in Fig. 6]) close to the bridge bonds in diborane, as well as the shorter B—B distances (1.687 Å in **6** vs. 1.751 Å in B_2H_6), characterize the strong B—H—B bridge. The $3c$-$2e$ B—H—B bonding in **6** is also supported by the natural bond orbital analysis (NBO)[27] and the significant B—H—B (0.580 and 0.370) and B—B (0.499) WBIs as compared to those in diborane. The tendency of another terminal hydrogen in **6** to form a B—H—B bridge (leading to **5**) is indicated from the elongated B–H distance (1.224 Å, Fig. 6) and the smaller WBI (0.822), in comparison to the terminal B–H bonds (1.178 Å with the WBIs around 0.970).

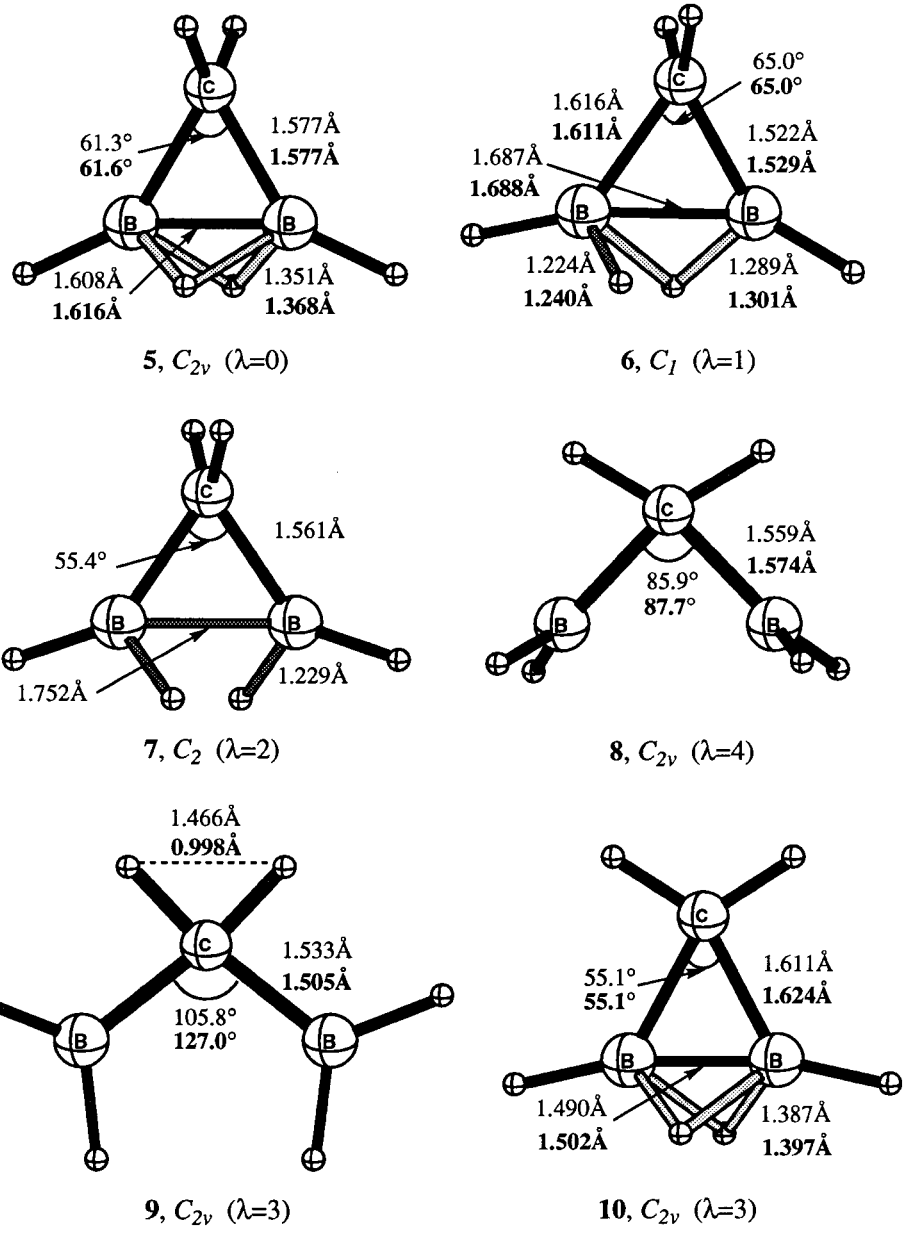

FIGURE 6. MP2(full) / 6–31G** and Becke3LYP / 6–311+G** (in bold) optimized geometries (bond length in Ångströms and bond angles in degrees) for **5**–**10**.

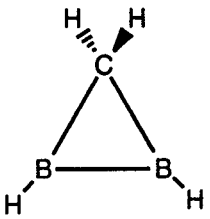

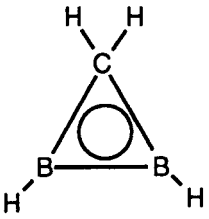

Planar Tetracoordinate Carbon

Hoffmann, Alder, and Wilcox first pointed out that planar tetracoordinate carbon would be stabilized by σ-donor and π-acceptor substituents.[11a] The best *ab initio* computations that employ large basis sets and include electron correlation effects predict that square planar methane is 130.5 kcal/mol higher in energy than tetrahedral methane.[11e] Although a planar C_{2v} form (with a three-center HCH bond) is somewhat more stable (121.6 kcal/mol above methane), this was also characterized as a higher order stationary point. Boron substituents[11] proved to be effective in stabilizing the planar methane. This was demonstrated computationally, e.g., in $C(BH_2)_4$[11a,b] and in the three-membered ring with two BH groups as shown below.[11c] Although the planar arrangement was computed to be 18.8 kcal/mol (at MP2/6−31G*) favored over the alternate ''tetrahedral'' form, neither of these structures were minima.[11d]

We have now examined structures **8**−**10** with planar tetracoordinate carbon arrangements in this context. Indeed, the two coplanar BH_2 substituents in **9** reduce the planar−tetrahedral (**4**) difference to 52.0 kcal/mol; note that **9** is a transition structure ($\lambda = 1$) at B3LYP and is also structurally quite different. While the dissociation of methane requires less energy than its planarization,[11e] the opposite is true for **9**. The π effects of the planar BH_2 groups in **9** are also shown by the 53.2 kcal/mol stabilization as compared to **8** (which has perpendicular BH_2s). The other planar tetracoordinate carbon structure, **10**, with a cyclic arrangement is 76.7 kcal/mol less stable than its tetrahedral counterpart, **5** (Table I). However, **10** has $\lambda = 3$ and is not a viable chemical entity.

Conclusions

At MP2, the barrier to conrotation in diborylmethane is considerably larger (1.9 kcal/mol) than for disrotation (0.1 kcal/mol). However, both the disrotation and conrotation in diborylmethane are correlated. Thus, the potential function describing the internal BH_2 rotations in $H_2BCH_2BH_2$ is inherently 2-dimensional rather than 1-dimensional. The total distribution of the critical points and the topology of the rotational PES are consistent with the Morse inequalities. Hence, both rotations need to be considered simultaneously to calculate the exact vibrational spectra. The hyperconjugation energy in diborylmethane (**1**−**4**) evaluated using ODP is around 12 kcal/mol. The dimerization of H_3CBH_2 leading to **1** is 5.6 kcal/mol exothermic. The 1,3 H exchange of **1** is a nonsynchronous process occurring via an unsymmetrical TS **6** and intermediate **5** with a 9.2 kcal/mol barrier. Structures **8**−**10** with ''planar tetracoordinate'' carbon are high energy hypothetical species, but **8** is a transition structure (at B3LYP) for the planar inversion of **1**.

Acknowledgment

R. M. M. thanks INTAS (Grant 94-0427) and the Russian Education ministry (Grant 95-0-9.1-70) for financial support. W. Q. and P. v. R. S. thank the Deutsche Forschungsgemeinschaft for funding. Y. M. and G. S. acknowledge the award of postdoctoral fellowships by the Alexander von Humboldt Foundation.

References

1. (a) R. B. Woodward and R. Hoffmann, *J. Am. Chem. Soc.*, **87**, 4389 (1965); (b) R. B. Woodward and R. Hoffmann, *Angew. Chem. Int. Ed. Engl.*, **8**, 781 (1969); (c) R. B. Woodward and R. Hoffmann, *The Conservation of Orbital Symmetry*, Academic Press, New York, 1969; (d) K. N. Houk, Y. Li, and J. D. Evanseck, *Angew. Chem. Int. Ed. Engl.*, **31**, 682 (1992).
2. K. B. Wiberg and R. E. Rosenberg, *J. Am. Chem. Soc.*, **112**, 1509 (1990).
3. B. R. Arnold, V. Balaji, and J. Michl, *J. Am. Chem. Soc.*, **112**, 1808 (1990).
4. H. Guo and M. Karplus, *J. Chem. Phys.*, **94**, 3679 (1991).
5. L. M. Stephenson, R. V. Gemmer, and J. I. Brauman, *J. Am. Chem. Soc.*, **94**, 8620 (1972).
6. (a) W. Koch, B. Liu, and P. v. R. Schleyer, *J. Am. Chem. Soc.*, **111**, 3479 (1989); (b) P. v. R. Schleyer, W. Koch, B. Liu, and U. Fleisher, *J. Chem. Soc., Chem. Commun.*, 1098 (1989); (c) W. Klopper and W. Kutzelnigg, *J. Phys. Chem.*, **94**, 5625 (1990).
7. Y. Yamaguchi and H. F. Schaefer III, *J. Am. Chem. Soc.*, **106**, 5115 (1984).

8. R. S. Grev, H. F. Schaefer III, and P. P. Gaspar, *J. Am. Chem. Soc.*, **113**, 5638 (1991).
9. M. Rosi, C. W. Bauschlicher, Jr., S. R. Langhoff, and H. Partridge, *J. Phys. Chem.*, **94**, 8656 (1990).
10. J. D. Dill, P. v. R. Schleyer, and J. A. Pople, *J. Am. Chem. Soc.*, **98**, 1663 (1976).
11. (a) R. Hoffmann, R. W. Alder, and C. F. Wilcox, Jr., *J. Am. Chem. Soc.*, **92**, 4992 (1970); (b) J. B. Collins, J. D. Dill, E. D. Jemmis, Y. Apeloig, P. v. R. Schleyer, R. Seeger, and J. A. Pople, *J. Am. Chem. Soc.*, **98**, 5419 (1976); (c) K. Krogh–Jesperson, D. Cremer, D. Poppinger, J. A. Pople, P. v. R. Schleyer, and J. Chandrasekhar, *J. Am. Chem. Soc.*, **101**, 4843 (1979); (d) E. D. Jemmis, G. Subramanian, and G. N. Srinivas, *J. Am. Chem. Soc.*, **114**, 7939 (1992); (e) M. J. A. Pepper, I. Shavitt, P. v. R. Schleyer, M. N. Glukhovtsev, R. Janoshek, and M. Quack, *J. Comput. Chem.* **16**, 207 (1995); (f) K. Sorger and P. v. R. Schleyer, *J. Mol. Struct.* (*Theochem.*), **338**, 317 (1995).
12. K. Lammertsma, O. F. Güner, A. F. Thibodeaux, and P. v. R. Schleyer, *J. Am. Chem. Soc.*, **111**, 8995 (1989).
13. M. J. Frisch, G. W. Trucks, H. B. Schlegel, P. M. W. Gill, B. G. Johnson, M. A. Robb, J. R. Cheeseman, T. Keith, G. A. Petersson, J. A. Montgomery, K. Raghavachari, M. A. Al-Laham, V. G. Zakrzewski, J. V. Ortiz, J. B. Foresman, J. Cioslowski, B. B. Stefanov, A. Nanayakkara, M. Challacombe, C. Y. Peng, P. Y. Ayala, W. Chen, M. W. Wong, J. L. Andres, E. S. Replogle, R. Gomperts, R. L. Martin, D. J. Fox, J. S. Binkley, D. J. Defrees, J. Baker, J. P. Stewart, M. Head–Gordon, C. Gonzalez, and J. A. Pople, *Gaussian 94, Rev. C.3*, Gaussian Inc., Pittsburgh, PA, 1995.
14. (a) W. J. Hehre, L. Radom, P. v. R. Schleyer, and J. A. Pople, *Ab Initio Molecular Orbital Theory*, Wiley, New York, 1986; (b) J. B. Foresman and Æ Frisch. *Exploring Chemistry with Electronic Structure Methods. A Guide to Using Gaussian*, 2nd ed., Gaussian Inc., Pittsburgh, PA, 1996.
15. (a) J. A. Pople, J. S. Binkley, and S. Seeger, *Int. J. Quantum Chem. Quantum Chem. Symp.*, **10**, 1 (1976); (b) C. Lee, W. Yang, and R. G. Parr, *Phys. Rev. B*, **37**, 785 (1988); (c) A. D. Becke, *Phys. Rev. A*, **38**, 3098 (1988); (d) A. D. Becke, *J. Chem. Phys.*, **98**, 5648 (1988).
16. P. Pulay, In *Ab Initio Methods in Quantum Chemistry*, K. P. Lawley, Ed., Wiley, New York, 1987, p. 241.
17. (a) J. A. Pople, A. P. Scott, M. W. Wong, and L. Radom, *Isr. J. Chem.*, **33**, 345 (1993); (b) A. P. Scott and L. Radom, *J. Phys. Chem.*, **100**, 16502 (1996) and references therein.
18. (a) R. M. Minyeav, *Int. J. Quantum Chem.*, **49**, 105 (1994); (b) R. M. Minyeav and D. J. Wales, *Chem. Phys. Lett.*, **218**, 3413 (1994); *J. Chem. Soc. Faraday Trans.*, **90**, 1831 (1994).
19. (a) K. Fukui, *Acc. Chem. Res.*, **14**, 363 (1981); (b) B. A. Ruf and W. H. Miller, *J. Chem. Soc. Faraday Trans. II*, **84**, 1523 (1988); (c) D. Heidrich, W. Kliesch, and W. Quapp, *Properties of Chemically Interesting Potential Energy Surfaces*, Springer, Berlin, 1991.
20. D. Heidrich and W. Quapp, *Theor. Chim. Acta*, **70**, 89 (1986).
21. J. Milnor, *Morse Theory*, Princeton University Press, Princeton, NJ, 1963.
22. I. G. Csizmadia, In *Symmetries and Properties of Non-Rigid Molecules: A Comprehensive Survey. Studies in Physical and Theoretical Chemistry 23*, J. Maruani and J. Serre, Eds., Elsevier, Amsterdam, 1983, p. 323.
23. Y. Mo and Z. Lin, *J. Chem. Phys.*, **105**, 1046 (1996).
24. For the isoelectronic $C_3H_6^{2+}$, the term *bishyperconjugation*, which is defined as the combined hyperconjugative effect on the same C—H bond(s) by two adjacent cation centers, was used. Also refer to P. Du, D. A. Hrovat, and W. T. Borden, *J. Am. Chem. Soc.*, **110**, 3405 (1988). Also see Ref. 12.
25. R. Köster, G. Seidel, B. Wrackmeyer, D. Bläser, R. Boese, M. Bühl, and P. v. R. Schleyer, *Chem. Ber.*, **124**, 2715 (1991).
26. (a) L. Hedberg, K. Hedberg, D. A. Kohler, D. M. Ritter, and V. Schomaker, *J. Am. Chem. Soc.*, **102**, 3430 (1980); (b) F. A. Cotton and G. Wilkinson, *Advanced Inorganic Chemistry*, 5th ed., Wiley, New York, 1988; (c) K. B. Wiberg and C. M. Breneman, *J. Am. Chem. Soc.*, **112**, 8765 (1990).
27. A. E. Reed and F. Weinhold, *Chem. Rev.* **88**, 899 (1988).